



HAL
open science

Atmospheric drivers of rainfall events in the Republic of Djibouti

Moussa Mohamed Waberi, Pierre Camberlin, Benjamin Pohl, Omar Assowe Dabar

► **To cite this version:**

Moussa Mohamed Waberi, Pierre Camberlin, Benjamin Pohl, Omar Assowe Dabar. Atmospheric drivers of rainfall events in the Republic of Djibouti. *International Journal of Climatology*, 2023, 43 (16), pp.7915-7934. 10.1002/joc.8299 . hal-04283410

HAL Id: hal-04283410

<https://hal.science/hal-04283410>

Submitted on 13 Nov 2023

HAL is a multi-disciplinary open access archive for the deposit and dissemination of scientific research documents, whether they are published or not. The documents may come from teaching and research institutions in France or abroad, or from public or private research centers.

L'archive ouverte pluridisciplinaire **HAL**, est destinée au dépôt et à la diffusion de documents scientifiques de niveau recherche, publiés ou non, émanant des établissements d'enseignement et de recherche français ou étrangers, des laboratoires publics ou privés.

Atmospheric drivers of rainfall events in the Republic of Djibouti

Moussa Mohamed Waberi^{1,2}  | Pierre Camberlin¹  | Benjamin Pohl¹  | Omar Assowe Dabar² 

¹Centre de Recherches de Climatologie, UMR 6282 Biogéosciences, CNRS/Université de Bourgogne, Dijon, France

²Observatoire Régional de Recherche sur l'Environnement et le Climat (ORREC), Centre d'Etudes et de Recherche de Djibouti (CERD), Djibouti-ville, Djibouti

Correspondence

Moussa Mohamed Waberi, Centre de Recherches de Climatologie, UMR 6282 Biogéosciences, CNRS/Université de Bourgogne, Dijon, France.
Email: moussamed1994@gmail.com

Funding information

Centre d'Etudes et de Recherches de Djibouti (CERD); Campus France (French government doctoral scholarship)

Abstract

The Republic of Djibouti is a small country in an arid context coupled with a high variability of rainfall that generates flash floods causing severe damage to the population and infrastructure. The mechanisms controlling extreme rainfall events in this part of the Horn of Africa remain poorly understood. In this study, we document the atmospheric circulation patterns associated with such events. To that end, we use rain-gauge data (a network of 36 stations on the period 2013–2020), satellite-based rainfall estimates (CHIRPS, IMERG, MSWEP and RFE) and atmospheric reanalyses (ERA5), all at the daily time-scale, over their common period 2001–2020. A multivariate Agglomerative Hierarchical Clustering of rainy days in Djibouti ($\geq 10\%$ of grid-points exceeding $1 \text{ mm}\cdot\text{day}^{-1}$, according to all four satellite products) reveal four clusters, which differentiate from each other by the intensity and spatial extent of rainfall. These clusters show a nonhomogeneous seasonal distribution, occurring mainly in the March–April–May (MAM) and July–August–September (JAS) seasons, and more rarely in October–November–December (OND). The atmospheric circulation anomalies associated with the clusters are quite similar and highly season-dependent. In MAM most clusters display an anomalous trough over the Red Sea, from 700 to 200 hPa. In JAS, an anomalous low over the southern Red Sea drives a thicker than normal monsoon flow at 700 hPa, while upper northerlies prevail at 200 hPa. In OND, most rainy events result from moisture advection from the Western Indian Ocean, favoured by positive phases of the Indian Ocean Dipole. Some highly unusual atmospheric circulation patterns (e.g., associated with tropical cyclones) can also result in intense rainfall events in Djibouti. These findings provide new insights on the physical causes of extreme events in the Horn of Africa, with applications to improved early warning and skill evaluation of climate models for climate change projections.

KEYWORDS

atmospheric circulation, Djibouti, rainfall events, satellite rainfall estimates

This is an open access article under the terms of the [Creative Commons Attribution](https://creativecommons.org/licenses/by/4.0/) License, which permits use, distribution and reproduction in any medium, provided the original work is properly cited.

© 2023 The Authors. *International Journal of Climatology* published by John Wiley & Sons Ltd on behalf of Royal Meteorological Society.

1 | INTRODUCTION

The Republic of Djibouti is a small country in the Horn of Africa, known for its arid climate (Nicholson, 2014; UNDP/UNSO, 1997), with erratic rains and no well-defined rainy seasons (Nicholson, 1996, 2017). Several reports (Ozer & Mahamoud, 2013; République de Djibouti, 2011) emphasized the enhanced arid conditions of the recent decades resulting in cattle mortality, water shortages, food insecurity and rural out-migration. They estimated that the 2008–2011 droughts caused an estimated 3.9% loss in the 4-year gross domestic product of the country. The eastern coastal region of the Republic of Djibouti was the most affected by the increased drought incidence in recent decades, with more than 80% of the extremely and severely dry events ($SPI-12/SPEI-12 < -1.5$) of the 1961–2021 period occurring during 2007–2017 (Assowe Dabar et al., 2022). By contrast, many examples can be found of days with very high precipitation in Djibouti City, which caused severe flash floods and widespread destruction (Cherel et al., 2020; Said Chiré, 2015). Cases of short-lived precipitation events resulting in major flooding include 7 April 1989 (180 mm), 12 April 2004 (93 mm), 23 November 2019 (155 mm) and 20 May 2018 (110 mm) when tropical cyclone Sagar hit the country. However, most of the atmospheric patterns driving intense to extreme wet events in the Republic of Djibouti are still unknown.

Many studies document interannual rainfall variations in the Greater Horn of Africa (GHA), with reviews available in Camberlin (2018) or Palmer et al. (2023), but little information is available on high-frequency (daily) rainfall variations and their atmospheric drivers. Some studies focusing on winter and spring/autumn transition seasons in Ethiopia, Eritrea and the Arabian Peninsula highlight the role of tropical–extratropical interactions, though it is uncertain whether their conclusions can be extrapolated to the Republic of Djibouti area. Habtemichael and Pedgley (1974) found that the origin of spring rains (April 1970) in Eritrea is a strong southward bend in the subtropical jet stream to $10^{\circ}N$ that provided a mechanism for the temporary development of deep convection clouds, fed by moisture from lower tropospheric southeasterly winds flowing across the southern Red Sea. de Vries et al. (2016) investigated the synoptic-scale dynamics of three extreme precipitation events that occurred in Saudi Arabia (in autumn, winter and spring) and found that all three cases involved strong tropical–extratropical interactions, whereby midlatitude forcing instigated an incursion of tropical moisture over the Arabian Peninsula that fuelled the heavy rainfall. Bekele-Biratu et al. (2018) studied sub-seasonal variability of the Belg rains (February–May rainfall season) in Ethiopia and found that the interactions

between extratropical and tropical systems across the Red Sea region play a major role in modulating the rainfall pattern during this season. Samman and Gallus Jr. (2018) investigated the synoptic patterns associated with the development of heavy rainfall in five different regions of Saudi Arabia. The study summarizes six major synoptic features, the most important of which is the Red Sea Trough (RST). The RST was found to substantially influence the precipitation in the country through the fall, winter and spring seasons, by advecting moisture from the Red Sea and the Arabian Sea towards the north. Atif et al. (2020) described extreme precipitation events (EPEs) over Saudi Arabia during the wet season and their associated teleconnections. They found that EPEs there are associated with midlatitude circumglobal wave trains (CGT), which evolve a few days before the onset of EPEs and decay afterwards. Ding and Wang (2005) and Saeed et al. (2011) demonstrated that the CGT influences boreal summer regional climates by modulating the Indian summer monsoon.

A notable feature is the paucity of studies documenting intense precipitation events or spells in the June–September (JJAS) season over the GHA as a whole, and Djibouti in particular. Contrary to West Africa where mesoscale convective systems (MCS) often associated with easterly waves explain a large proportion of the intense rainfall events, no organized disturbances have been clearly identified so far in the GHA during the JJAS season, as easterly waves can hardly be traced back east of $30^{\circ}E$ (Jury, 2011; Mekonnen & Rossow, 2018). In a part of the GHA which is very wet in summer, Jury (2011) studied the meteorological scenario of Ethiopian floods in 2006–2007 and found that most extreme events (in July of 2006 and July of 2007) were associated with anomalously strong southerly monsoon flow over the western Indian Ocean. The Djibouti area is much drier in summer, but Jury (2016) described a convective outbreak over the southern Red Sea which leads to the initiation of easterly waves and extreme precipitation events over West Africa.

Tropical depressions and tropical cyclones develop over the Arabian Sea in two separate seasons (May–June and October–December), but those reaching the coasts of the Arabian Peninsula and Northeastern Africa are a rarity (Terry & Gienko, 2019). Several works analysed the statistical distribution of tropical cyclones over the Arabian Sea (Evan & Camargo, 2011; Tiwari et al., 2022), but very few of them documented those which affected its westernmost part (Cherel et al., 2020), and none studied statistically their contribution to rainfall over the land areas running from eastern Somalia to Yemen.

Among the previous studies dedicated to the analysis of intense climate events over the complex region of the GHA, none are at the scale of small, vulnerable territories

like the Republic of Djibouti. The few studies done on the region and on the Arabian Peninsula show that the atmospheric mechanisms of rainfall are of at least three different types (tropical–temperate interactions, convective outbreaks, tropical cyclones) and are more or less organized depending on the season and the type of drivers. Since it is unknown if the conclusions of those studies can be extrapolated to Djibouti, the objective of this paper is to document the atmospheric mechanisms behind the intense rainfall recorded there. To that end, the space–time patterns of daily rainfall distribution are analysed in order to document the spatial extent and the seasonal variations of the rain events in the country. Then, the atmospheric circulation anomalies associated with the rainfall events are extracted on a seasonal basis.

2 | DATA AND METHODOLOGY

2.1 | Description of the study area

The Republic of Djibouti is a small country (23,200 km²) located near the southern extremity of the Red Sea in the Horn of Africa. It is geographically bounded by latitudes 11°–12.5°N and longitudes 42°–43.5°E and bordered by Eritrea to the north, Ethiopia to the west and south, Somalia to the southeast, and it faces the Red Sea and the Gulf of Aden to the east (Figure 1). The country has two seasons: a relatively cold season (October–April) and a hot season (May–September) (Beau et al., 1976). The mean annual precipitation of Djibouti (150 mm·year⁻¹) is under 10% of the mean annual potential evapotranspiration (2000 mm·year⁻¹; Houmed-Gaba, 2009). This led to classify the local climate as arid (UNDP/UNSO, 1997). The annual accumulation of precipitation in the Republic of Djibouti is influenced by the elevation and the proximity to the Indian Ocean (Assowe Dabar et al., 2021). A maximum rainfall is observed in mountainous areas of the Tadjourah district such as Randa (240–300 mm·year⁻¹), while lower annual precipitation is found in low altitude zones such as Moulhoulé and Khor Angar (northeast of Djibouti, with less than 60 mm·year⁻¹).

In Djibouti, the rainfall regime displays multimodal patterns. Despite the low annual rainfall amounts, Djibouti exhibits a strong spatial differentiation in terms of rainfall regimes. The regionalization of long-term monthly rainfall data (1946–2017) identified two main seasonal rainfall regimes (EAST and WEST) across the Republic of Djibouti (Abdou, 1990; Assowe Dabar et al., 2021). The western seasonal rainfall regime presents two peaks, the first one in MAM, hypothesised to be mostly associated with tropical–temperate interactions, as in neighbouring northeastern Ethiopia (Bekele-Biratu et al., 2018) and

Yemen (de Vries et al., 2016), and the second one in JJAS, associated with the summer monsoon, albeit its reduced activity over Djibouti due to its location in the lee of the Ethiopian Highlands (Flohn, 1965; Pedgley, 1966). The eastern seasonal rainfall regime also has two peaks, the first one in MAM (just like the western regime) and the second one in OND as part of the “short rains” of equatorial East Africa (Camberlin, 2018; Yang et al., 2015).

2.2 | Data sources

In this study we used three different types of datasets: observed rain gauge data, merged satellite rain-gauge products and reanalyses.

2.2.1 | Observational rainfall data

An unpublished network of 36 rain-gauge stations commissioned in 2013 by the National Meteorological Agency of Djibouti (ANM) with daily rainfall data was used in this work. This network of stations (see their location in Figure 1) is quite representative of the different parts of the country, including the East–West differentiation noted above in the annual rainfall regimes. A quality control was performed on the observed data to detect outliers and systematic errors. The data cover the period 2013–2021, over which the data availability rate is at least 62.7% (Dorra) and peaks at 90.7% (Ali-Sabieh). Various data gaps occur during the period September 2016–December 2020, with a gap rate of 26.9% at all stations (Figure S1, Supporting Information). Stations in the northern regions (Tadjourah and Obock) have larger gaps (50.9%) compared to those in the southern regions (Dikhil, Arta, Ali-Sabieh and Djibouti with 16.3%).

Given the shortness of the record, this data set is used only to evaluate the quality of gridded merged satellite-rain-gauge products, and to assess the realism of the clusters of daily rainfall events based on these products.

2.2.2 | Merged satellite rain-gauge products

A selection of four satellite-based rainfall estimates products is proposed in this study (Table 1). These products were selected because they are among the most efficient in the East African region (Cattani et al., 2020; Dinku et al., 2018; Gebrechorkos et al., 2018; Kimani et al., 2017), but also due to their high spatial resolutions (ranging from 0.05° to 0.1° in latitude/longitude), which makes them suitable for a small area like the Republic of

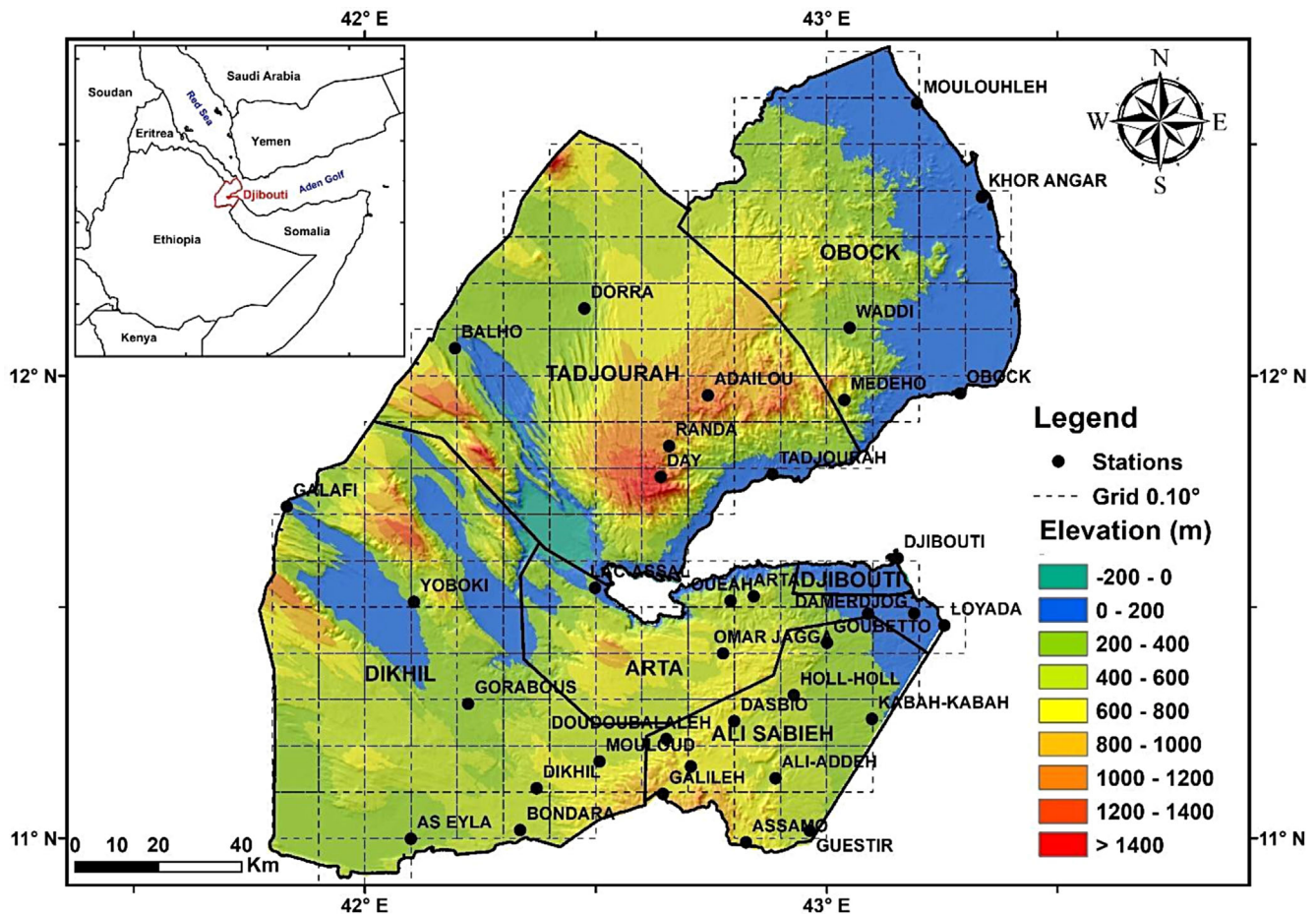


FIGURE 1 Location and elevation map of the Republic of Djibouti. The black dots and the grid represent respectively the rain stations and the spatial resolution of the satellite products used in this work [Colour figure can be viewed at [wileyonlinelibrary.com](https://onlinelibrary.wiley.com/doi/10.1002/joc.8299)]

Djibouti. In addition to satellite information, these products incorporate observed data (over the country only Djibouti Airport station is available for calibration in any of the rainfall estimate products that use observation as input data), and one of them (MSWEP) also includes reanalysis data.

The Climate Hazard Group Infrared Precipitation with Stations version 2 (CHIRPS) is a quasi-global (ranging from 50°S to 50°N and all longitudes) gridded rainfall data source with a spatial resolution of 0.05° (~5 km) at daily to monthly timescales since 1981. This dataset is mainly designed for monitoring droughts and other global environmental changes in data scarce regions like East Africa. Due to its high spatial and temporal resolutions and its extensive quality control, CHIRPS is widely used for assessing long-term rainfall variability and trends in climate (Assowe Dabar et al., 2021; Williams et al., 2012). More details of the product can be found from Funk et al. (2015).

Rainfall Estimates v.2 (RFE) is a daily climatology dataset centred over Africa (40°S–40°N and 20°W–55°E) with a spatial resolution of 0.1° starting in 2001 and updated in near real-time (within 2 days; Xie & Arkin, 1996). The

dataset guarantees a historical consistency over the whole time period, allowed by the use of a single retrieval algorithm based on calibrated 3-hourly infrared satellite.

Integrated Multi-Satellite Retrieval for Global Precipitation Measurement v.6 (IMERG) is a global gridded rainfall data source with a spatial resolution of 0.1° (~10 km), available at a daily timescale since June 2000 and a data latency of about 3.5 months. More details on the product can be found from Tan et al. (2019).

Multi-Source Weighted Ensemble Precipitation v.2.8 (MSWEP) is a global gridded rainfall data source with a 3-hourly 0.1° (~10 km) spatial resolution available from 1979 to present. MSWEP incorporates daily gauge observations, satellite and reanalysis estimates (Beck et al., 2017, 2019). Although this dataset incorporates several existing rainfall estimate products, it is unsure whether it necessarily improves rainfall estimates upon individual precipitation products over a poorly sampled area such as the Republic of Djibouti.

In this work, the four rainfall estimate products were analysed over their common period of data availability, 2001–2020.

TABLE 1 Main characteristics and references of some precipitation datasets

Acronym	Full name	Data source	Temporal coverage	Temporal resolution	Spatial coverage	Spatial resolution	Latency	References
CHIRPS v.2	Climate Hazards Group InfraRed v.2	S, G	1981–present	Daily	Global	0.05°	1 month	Funk et al. (2015)
IMERG v.6	Integrated Multi-satellite Retrieval for Global Precipitation	S, G	June 2000–present	Half-hourly	Global	0.1°	3.5 months	Tan et al. (2019)
MSWEP v.2.8	Multi-Source Weighted Ensemble Precipitation v.2.8	S, G, R	1979–2020	3 h	Global	0.1°	Few months	Beck et al. (2017, 2019)
RFE v.2	Rainfall Estimates v.2	S, G	2001–present	Daily	Africa	0.1°	2 days	Xie and Arkin (1996)

Note: In the data source column, S, R and G, stands for satellite, reanalysis and gauge information, respectively.

2.2.3 | Reanalysis data

This study uses the ERA5 atmospheric reanalysis (Copernicus Climate Change Service, 2017; Hersbach et al., 2020), that is, the fifth generation of the European Centre for Medium-Range Weather Forecasts (ECMWF) atmospheric reanalysis of the global climate. ERA5 combines vast amounts of historical observations into global estimates using advanced modelling and data assimilation systems. It provides hourly estimates of a large number of atmospheric, land and oceanic climate variables. The data cover the Earth on a 0.25° (~30 km) grid, with 137 levels from the surface up to a height of 80 km, from 1940 to present (restricted to 2001–2020 for this work). Here, we used several ERA5 atmospheric variables (geopotential height, specific humidity, air temperature, and the three components of the wind: zonal, meridional and vertical) at four different pressure levels (200, 500, 700 and 925 hPa). We also analysed total column precipitable water, outgoing longwave radiation flux (OLR) and vertically integrated moisture transport.

2.3 | Methodology

A first aim of this paper is to document the space–time patterns of daily rainfall distribution in Djibouti. Yet, the availability of observed precipitation data there is limited in time (2013–2021). To overcome this constraint, the identification and classification of rainfall events is based on satellite products (section 2.2.2) over their longer common period 2001–2020. The analysis consists of three steps: (i) a comparison between the different rainfall

datasets, (ii) a clustering of the rainfall events and (iii) a detection of the atmospheric patterns associated with the clusters.

The first step exploits the network of 36 rainfall stations and the above four satellite products (CHIRPS, IMERG, MSWEP and RFE). The general performance of these products to correctly detect the occurrence of rainy days ($P \geq 1$ mm) and the corresponding amount of rainfall is evaluated using standard statistical parameters, as in similar previous studies (e.g., Dinku et al., 2018 for eastern Africa; Camberlin et al., 2019 for Central Africa; Satgé et al., 2020 for West Africa). For rainfall occurrence, contingency table statistics include the accuracy (true positive events/all events), the true positive rate (or recall = true positive events/observed rainy events), the false positive rate (or fallout = false positive events/observed dry events), and the precision (true positive events/estimated rainy events). These statistics address complementary aspects of rain occurrence detection. For assessing the accuracy of the estimates while accounting for matches due to random chances, the Heidke skill score (HSS) is also computed, with a HSS of zero meaning no skill, and a HSS of 1 for a perfect accuracy. The observed and estimated rainfall amounts from the satellite products were compared using the Pearson coefficient of correlation (r), the mean bias error (MBE) and the root-mean-square error (RMSE).

All the comparisons are made between rain gauge data and their nearest grid points from each satellite product. As we seek to exclude local showers, only the days with at least 10% of stations across the Republic of Djibouti recording a minimum of 1 mm of rainfall are

retained. This approach is duplicated for each of the four rainfall products, separately (days with at least 10% of the grid points with each a minimum of 1 mm of rainfall). The satellite-estimated rain events are then analysed to assess whether they correctly detect the observed events over the common period 2013–2020. The analysis is then extended to the longer period (2001–2020) using satellite products only, since the observational times-series are too short to detect robust space–time patterns. Only the days where there is a consensus between the estimation products are retained.

As a second step, a cluster analysis of the daily rain events of the extended period (2001–2020, $N_1 = 7229$ days) is carried out in order to identify the most recurrent rainfall patterns in terms of spatial distribution and intensity across the Republic of Djibouti. To that end, all grid points data covering Djibouti from the four satellite products (after regridding CHIRPS data to 0.1° to match the spatial resolution of the three other products) are concatenated. A square root transformation is applied to this data in order to reduce the skewness of the daily rainfall distributions before normalizing the time-series separately for each satellite product and each grid-point. From this transformed dataset, a selection is made of the days where at least 10% of the grid points record (based on the raw data) a daily precipitation amount of at least 1 mm in each of the four satellite products ($N_2 = 768$ days). Agglomerative Hierarchical Clustering (AHC) is then applied to the concatenated data ($4 \times N_2 = 3072$ observations). In order to reduce uncertainties, only the days classified in the same cluster by at least three satellite products are retained ($N_3 = 541$ days). The mean precipitation and precipitation anomalies of the days in the different clusters are displayed below for each satellite product to characterize their spatial rainfall patterns. To assess the robustness of the clustering, the observed mean rainfall (spatial patterns and seasonal distributions) for each cluster is computed, taking a subsample of the N_3 days over the period for which rain-gauge data are available (2013–2020).

Finally, in order to document the atmospheric patterns associated with intense rainfall days in Djibouti, a composite analysis of the days associated with the different clusters is carried out, by (i) computing daily deseasonalized climate anomalies of the different ERA5 variables and (ii) computing the average climate anomalies for the different clusters with application of the Student's t test to highlight the significant anomalies. Because the background mean atmospheric circulation over the Republic of Djibouti strongly changes along the year, the last step is carried out on a seasonal basis.

3 | RESULTS AND DISCUSSION

3.1 | Comparison between observed rainfall and satellite rainfall estimates

The performance of the satellite products (CHIRPS, IMERG, MSWEP and RFE) in reproducing the intensity and frequency of daily observed rainfall ($P \geq 1$ mm) was evaluated in Table 2. All the stations and seasons are combined together ($N = 92,257$ observations). CHIRPS is the best product in the detection of dry days (which account on average for 95% of the days in Djibouti), as shown by the low value of fallout (7.7%). It is also the least biased product with an MBE of 0.18 mm overall 36 stations. IMERG presents the best balance between recall (rainy day detection) and fallout (false positive rate) as shown by the highest HSS (0.183) and precision (12.8%). MSWEP is the best among the four products in the detection of rainy days (recall = 72.7%), but it is the worst in the detection of dry days (fallout = 12.6%). It shows the highest correlation coefficient (r) and the lowest RMSE, suggesting a slightly better skill at reproducing rainfall amounts. Yet, RMSE values remain high for all products (typically, $6\text{--}7$ mm·day $^{-1}$), suggesting that rainfall amounts are not well estimated. However, this is partly related to the fact that gridded (areal) rainfall data tend to underestimate gauged (point) rainfall, especially in the case of extreme events. Finally, RFE does not stand out as the best performing product for any criterion, but still exhibits fair overall skills, and offers a coherence throughout the study period that does not exist in any other dataset.

Spatially, all statistical parameters indicate better performance of satellite products in the vicinity of Djibouti Airport station and worse performance in the remote regions (e.g., the far west and northeast; not shown). This is because Djibouti Airport is the only calibration point for satellite products in the Republic of Djibouti.

In order to exclude very localized rainfall, we consider hereafter a rain event as a day with at least 10% of the stations or grid points recording at least 1 mm of precipitation, provided that at least 90% of the rain gauges have available data for that day. Figure 2a illustrates the time distribution of such rainy events in the observed data and satellite products over the period 2013–2020. It aims at assessing how well the combined rainfall products reproduce the observed events and their seasonal distribution. Table 3 provides statistics on the matching between observed and satellite data depending on the season.

As observed in Figure 2 and Table 3, the wettest season is JJAS (mainly from July to September), with 46% of the observed events of which 98% were detected by at least one satellite product. The majority of these

detections (73%) are consensually made by all four products. The MAM and OND seasons have similar numbers of rainy events, respectively, 25% and 23%.

TABLE 2 Comparative statistics of daily rainfall frequency and intensity between observed data and satellite products over the Republic of Djibouti over the 2013–2020 period

	CHIRPS	IMERG	MSWEP	RFE
Accuracy	91.4%	91.4%	87.1%	89.7%
Recall	48.0%	58.7%	72.7%	52.2%
Fallout	7.7%	8.0%	12.6%	9.5%
Precision	11.0%	12.8%	10.3%	9.8%
HSS	0.153	0.183	0.151	0.137
<i>r</i>	0.10	0.13	0.16	0.09
MBE (mm·day ⁻¹)	0.18	0.34	0.27	0.45
RMSE (mm·day ⁻¹)	6.23	6.49	6.07	7.47

Note: In bold, the best performing satellite product for each skill score.

Almost all of these events (97% and 100%, respectively) are detected by at least one satellite product. Seventy-seven percent of these detections are made consensually in MAM against only 33% in OND. Finally, the JF season is the driest, with only 6% of the rain events. Thirty-eight percent of these days are detected by at least one satellite product, none of which is consensual.

We conclude from this analysis that large-scale rainy events are likely to occur throughout the year, but are unevenly distributed over the four seasons. While JF is the driest season, more rainy days are found in JJAS. During this season, wet days seem to run in an uninterrupted way for many consecutive days (Figure 2), but this is due to many localized convective showers which fall over scattered stations (not shown). Dry days over the whole country are therefore quite rare at that time. Other rain spells (especially in MAM) occur in short spells separated by longer spells of totally dry weather, suggesting a stronger synoptic control. The weaker consensus for rainfall detection in JF is probably due to a different nature

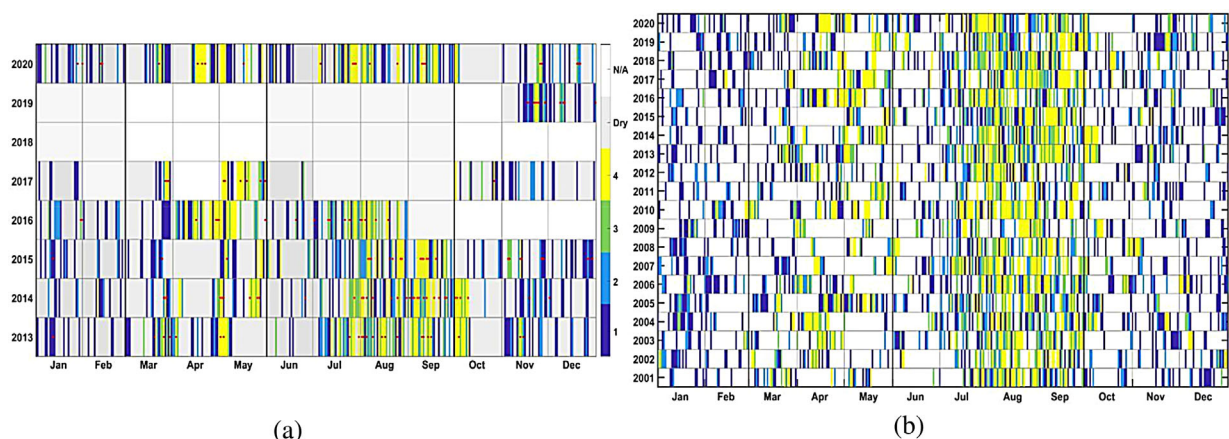


FIGURE 2 Temporal distribution of rain events (at least 10% of the grid points or stations with at least 1 mm) over the Republic of Djibouti in (a) observations and satellite products (2013–2020) and (b) satellite products only (2001–2020). Red dots (panel a) indicate observed rain events and shadings show rain events detected by satellite products (number of products in colour) [Colour figure can be viewed at wileyonlinelibrary.com]

TABLE 3 Seasonal distribution of observed rain events (at least 10% of the stations with at least 1 mm) detected and undetected by satellite products over the period 2013–2020

Season	Number of rainy days observed	Detected by 1 product	Detected by 2 products	Detected by 3 products	Detected by 4 products	Undetected
JF	8	3	0	3	0	2
MAM	36	3	3	2	27	1
JJAS	66	4	3	10	48	1
OND	33	6	8	8	11	0
All	143	16	14	23	86	4

Note: In bold, the largest number of observed rain events detected by a set of satellite products in each season.

of the rain-bearing systems at that time. While convective rains dominate in summer and during the transition seasons, rains associated with cold fronts prevail in winter (Beau et al., 1976), and are hypothesised to be more difficult to capture by satellite products, because they mostly rely on thermal infrared imagery. Testing this hypothesis is not our scope here, because the JF season includes a very small number of rainy events and will therefore be discarded from the seasonal analyses of rainfall events performed and discussed below.

Figure 2a shows that some events detected by the satellite products do not coincide with observed rainfall events. Overall, 42% (86 days) of the rain events detected simultaneously by all four satellite products correspond to observed rain events (“true positives”). This results in an apparently high number of “false positives” (119). However, 60% of those events recorded rainfall in at least one of the gauges but were discarded because of their smaller spatial extension (less than 10% of the rain gauges). It is likely that some of the remaining 40% could not be captured by the network (whose density is weaker in the western and northern parts of the country), because they were associated with small-scale convective cells.

Interestingly, the rate of true positives drops to 20.5%, 10.4% and 4.7%, respectively, for the simultaneous detection with 3, 2 and 1 satellite products, against 42% with the four products. These results illustrate the relevance of retaining only the events detected in a concordant way by a majority of the rainfall estimate products for further analysis.

3.2 | Multiproducts Agglomerative Hierarchical Clustering of rainy events

Agglomerative Hierarchical Clustering (AHC) was applied to the days when the four satellite products present simultaneously at least 10% of the grid points with 1 mm of precipitation (768 days), over their common period (2001–2020). Based on the Euclidean distance between the clusters (Figure 3), we chose to retain four clusters in the remainder of this work, and only the days classified in the same cluster by at least three satellite products (541 days). These choices appear as a good compromise to have a concise and yet robust view of the diversity of rainfall events, and ensure consistency between rainfall estimates. The corresponding rainy days are unevenly distributed in the four clusters: 8% of the days in cluster #1, 22% in cluster #2, 12% in cluster #3 and 58% in cluster #4. The monthly distributions of these days show strong similarities reflecting the dominant rainfall regimes over the country, with a main peak in

the mid- to late-summer (August–September) and a secondary one in spring (April or May). Few events occur in JF, slightly more in OND in some clusters.

Figure 4 shows the spatial distribution of mean precipitation and mean standardized precipitation anomalies for each satellite product and for each cluster. Cluster #1 is characterized by relatively heavy rainfall (13.5 mm on average across the four products) and high positive rainfall anomalies over the whole country. It is identified as the “intense cluster.” The patterns of rainfall anomalies in the four satellite products show the largest positive anomalies in the northern region and all around the Gulf of Tadjourah. CHIRPS and MSWEP show the influence of the topography, while IMERG and RFE produce more rain in the southern region of the country. These differences reflect the systematic biases that some of these products display over Djibouti (not shown). The cluster #1 events are rare and almost as numerous in the MAM as in the JJAS season, with peaks in April and August, respectively (Figure 3).

Cluster #2 (Figure 4) exhibits higher rainfall intensities and anomalies in the southwestern region of the country (and is therefore referred to as the “southwestern cluster”). The anomaly patterns are very consistent across the four products, in spite of some differences in the raw rainfall amounts due to the uneven biases of the products. The temporal distribution shows a major peak in July–September (Figure 3).

Cluster #3 (“eastern cluster”) is characterized by localized rainfall in the eastern regions of Djibouti. This includes the northeastern coast, where absolute rainfall amounts remain quite low, and the mountain ranges to the north of the Gulf of Tadjourah. Most occurrences are found in August and September, but this cluster can also be found until December on the one hand, and in April and May on the other hand (Figure 3).

Finally, cluster #4 (“moderate rainfall cluster”) is characterized by low-intensity rainfall and anomalies over the whole territory (spatially averaged rainfall of 1.4 mm across the four products). It mostly occurs between April and October, once again with a main peak in August and September.

The observed rainfall associated with the days ascribed to each cluster, but for the period 2013–2020 only, is plotted on Figure 5. Rainfall patterns are very similar to the satellite estimates: intense rainfall ($7.1 \text{ mm}\cdot\text{day}^{-1}\cdot\text{station}^{-1}$) over all stations for the intense cluster (#1), heavier rainfall in the southwest for the southwestern cluster (#2), more intense rainfall in the east for the eastern cluster (#3) and finally low rainfall ($0.7 \text{ mm}\cdot\text{day}^{-1}\cdot\text{station}^{-1}$) over all stations for the moderate rainfall cluster (#4). The monthly rainfall distributions well match those obtained from the four

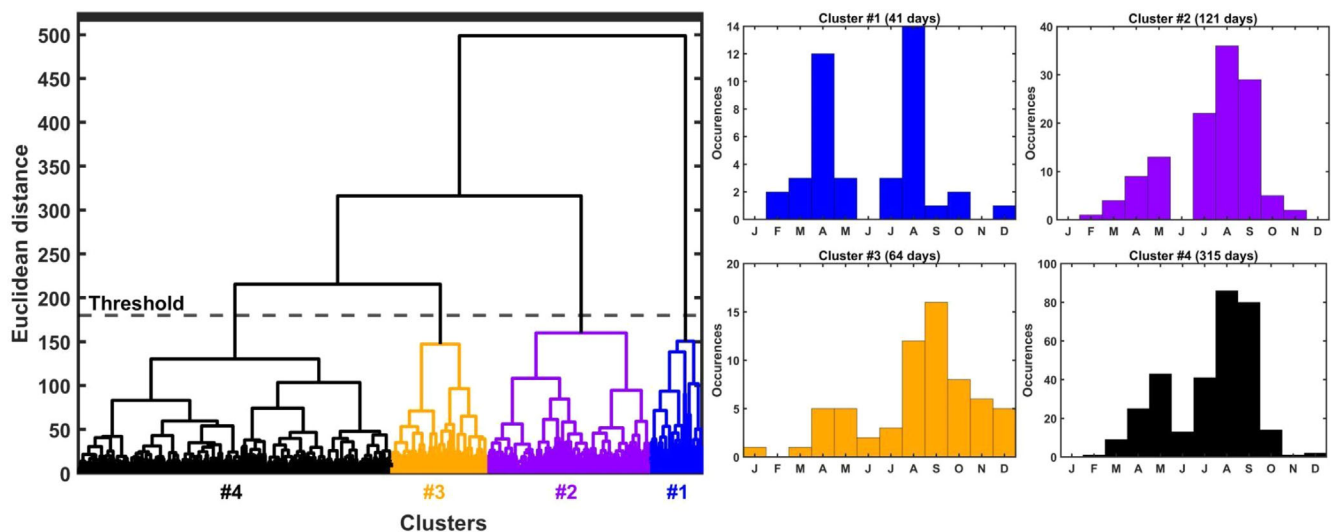


FIGURE 3 Multiproducts (CHIRPS, IMERG, MSWEP and RFE) Agglomerative Hierarchical Clustering of rain events in Djibouti over the period 2001–2020. The left panel shows the classification tree with the rainfall events (detected by the satellite products) on the x-axis and the Euclidean distances between them on the y-axis. The left panels show the monthly occurrence of the selected days of the four clusters [Colour figure can be viewed at [wileyonlinelibrary.com](https://onlinelibrary.com)]

clusters. This confirms the robustness of our methodology and the ability of the combined four products to reproduce the actual rainfall patterns over the country. There is also a good match between the satellite products and the observations for the four clusters in terms of rain events intensity and spatial extension of the rains (both are in decreasing order from cluster #1 to #4), but with positive biases in the satellite estimates especially in the spatial extension of rain events (Figure S2).

3.3 | Rain-bearing mechanisms

In this section, we document the atmospheric mechanisms associated with the rainfall events ascribed to each cluster. We split cluster occurrences by season because Djibouti and more globally the East African region show major seasonal changes in the background atmospheric circulation, in particular the monsoons reversal related to the shifts in the Hadley circulation (Camberlin, 2018).

3.3.1 | Mean atmospheric circulation

Figure 6 shows the seasonal mean wind patterns for different spatial domains (local, regional and large scale) and at different atmospheric levels (near surface: 925 hPa; mid-troposphere: 700 and 500 hPa; and upper troposphere: 200 hPa).

Locally (near Djibouti) during the JF, MAM and OND seasons at 925 hPa, easterly winds prevail, as part

of the trade winds from the northwestern Indian Ocean. These easterlies are channelled by the Gulf of Aden and Red Sea, resulting in southeasterlies along the Red Sea. The JJAS season is characterized by a complete low-level wind reversal. The main southwesterly monsoon flow heads towards the Indian subcontinent. It is connected to the African monsoon west of Ethiopia, which continues as a northwesterly flow along the Red Sea.

At 700 hPa a belt of easterlies/northeasterlies predominates, shifting northward from boreal winter to summer, but quite persistent over Djibouti. North of 18°–20°N, as part of the extratropical circulation, westerlies persist throughout the year, except in JJAS.

In the mid-troposphere (500 hPa), despite nuances, the atmospheric circulations for the JF, MAM and OND seasons are similar, with a steady subtropical jet stream centred around 30°N and a trough over the Arabian Peninsula. The same feature dominates in the upper troposphere (200 hPa). However, in JJAS, the westerlies weaken and shift northward. Easterly winds strengthen in the Tropics, taking the form of the strong Tropical Easterly Jet (JET) which blows over the Djibouti area from its origin in South Asia.

3.3.2 | Anomalous atmospheric circulation

In this subsection, in order to understand the atmospheric mechanisms that cause rainfall in the Republic of Djibouti, we analyse the anomalous atmospheric circulation for each cluster (except for the “moderate cluster” #4

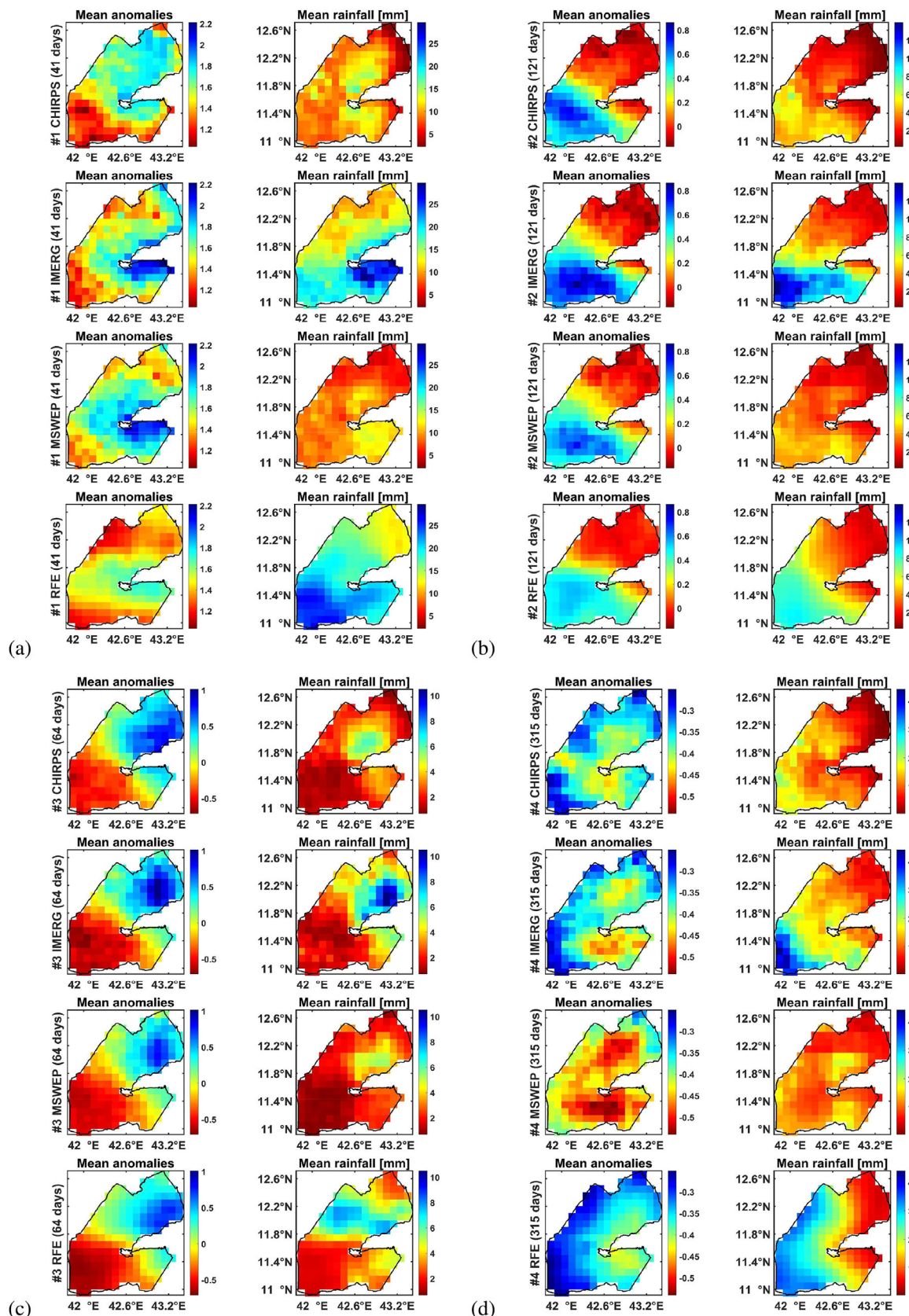


FIGURE 4 Spatial distribution of rainfall for the 4 clusters (panels a–d) in the satellite products over their common period 2001–2020. In each panel, the different rows correspond to the different satellite products and the columns show the standardized average rainfall anomalies (left column) and the average rainfall (right column, in mm) [Colour figure can be viewed at [wileyonlinelibrary.com](https://onlinelibrary.wiley.com/doi/10.1002/joc.8299)]

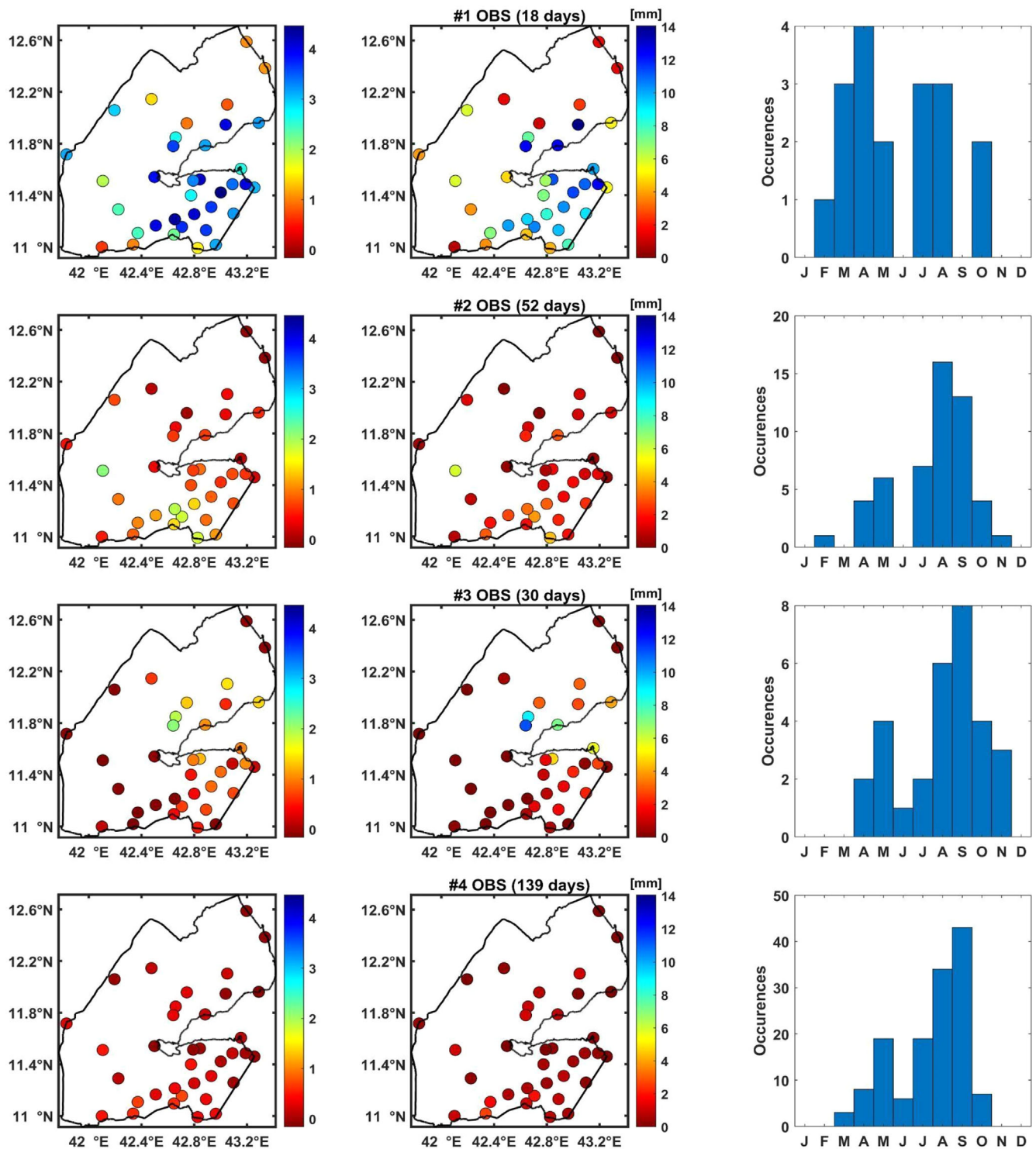


FIGURE 5 Spatial and temporal distribution of observed rainfall (2013–2020) for the days classified in each of the previous clusters. Each row corresponds to a different cluster and the columns (left to right) correspond respectively to the standardized average rainfall anomalies, average rainfall and the monthly occurrence of cluster days [Colour figure can be viewed at wileyonlinelibrary.com]

which is made up of very low-intensity, scattered rainfall events) and each season (except for the very dry JF season). Analysis concentrates on the 700 and 200 hPa pressure levels which are fairly representative of the mid and upper tropospheric circulations, respectively.

The 925-hPa pressure level is not analyzed due to the influence of the topography. It generally displays weaker and less consistent anomalies (Figure S3). While this study remains focused on the daily timescale, relationship between the interannual variations in the

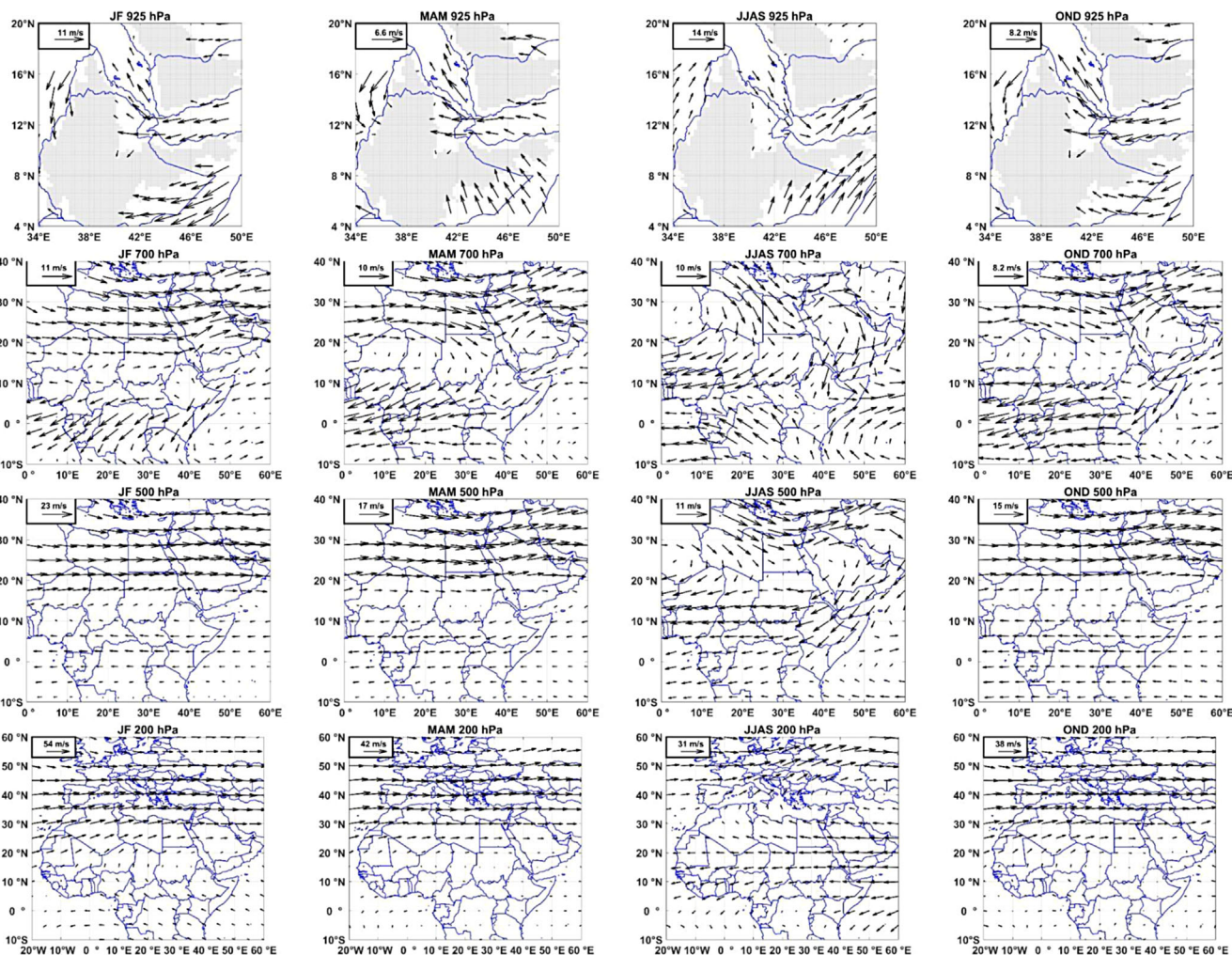


FIGURE 6 Seasonal mean wind fields ($\text{m}\cdot\text{s}^{-1}$) at different pressure levels (200, 500, 700 and 925 hPa) [Colour figure can be viewed at wileyonlinelibrary.com]

frequency of rain events (for each cluster) and large-scale drivers of tropical and extratropical circulations was also examined (ENSO [Niño3.4 index], Indian Ocean Dipole, North Atlantic Oscillation). Results were barely or non-significant (Figure S6 and Table S1), except where otherwise specified. Similarly, the distribution of the rain events with respect to the different phases of the Madden-Julian Oscillation (indices from Wheeler & Hendon, 2004) failed to show any robust and coherent pattern.

Figure 7 shows the significant anomalies of daily geopotential height and wind speed of the intense, southwestern and eastern clusters for three aforementioned seasons and at 700 hPa. Figure 8 shows the 200 hPa level. From a quick look, the atmospheric circulation anomalies appear more season dependent than cluster dependent.

In MAM, the three clusters show an anomalous trough over the central Red Sea from 700 to 200 hPa. It results in westerly to southwesterly wind anomalies in

both the mid- and upper-troposphere along its southern and eastern flanks, including over Djibouti. This Red Sea trough is part of a circumglobal wave train (CGT) identified by previous studies (e.g., Almazroui et al., 2018; Branstator, 2002; Ding & Wang, 2005; Saeed et al., 2011, 2014) which extends from the Arctic Ocean towards Europe and South Asia. This wave train shows well in the composites of Figures 7 and 8. The CGT modulates the midlatitude cyclone activity which brings cold air in the upper troposphere over Arabian Peninsula during wet seasons. Further, its pattern also facilitates upper air divergence through the jet stream, which helps to develop mesoscale convective systems (MCS) as discussed by Branstator (2002). The CGT accounts for a large portion of intense rainfall events in Saudi Arabia (Atif et al., 2020). Kiladis and Weickmann (1997) showed that in tropical regions located within upper westerlies, wave energy propagating from the midlatitudes drives convection ahead of upper-level troughs. Djibouti lies at the

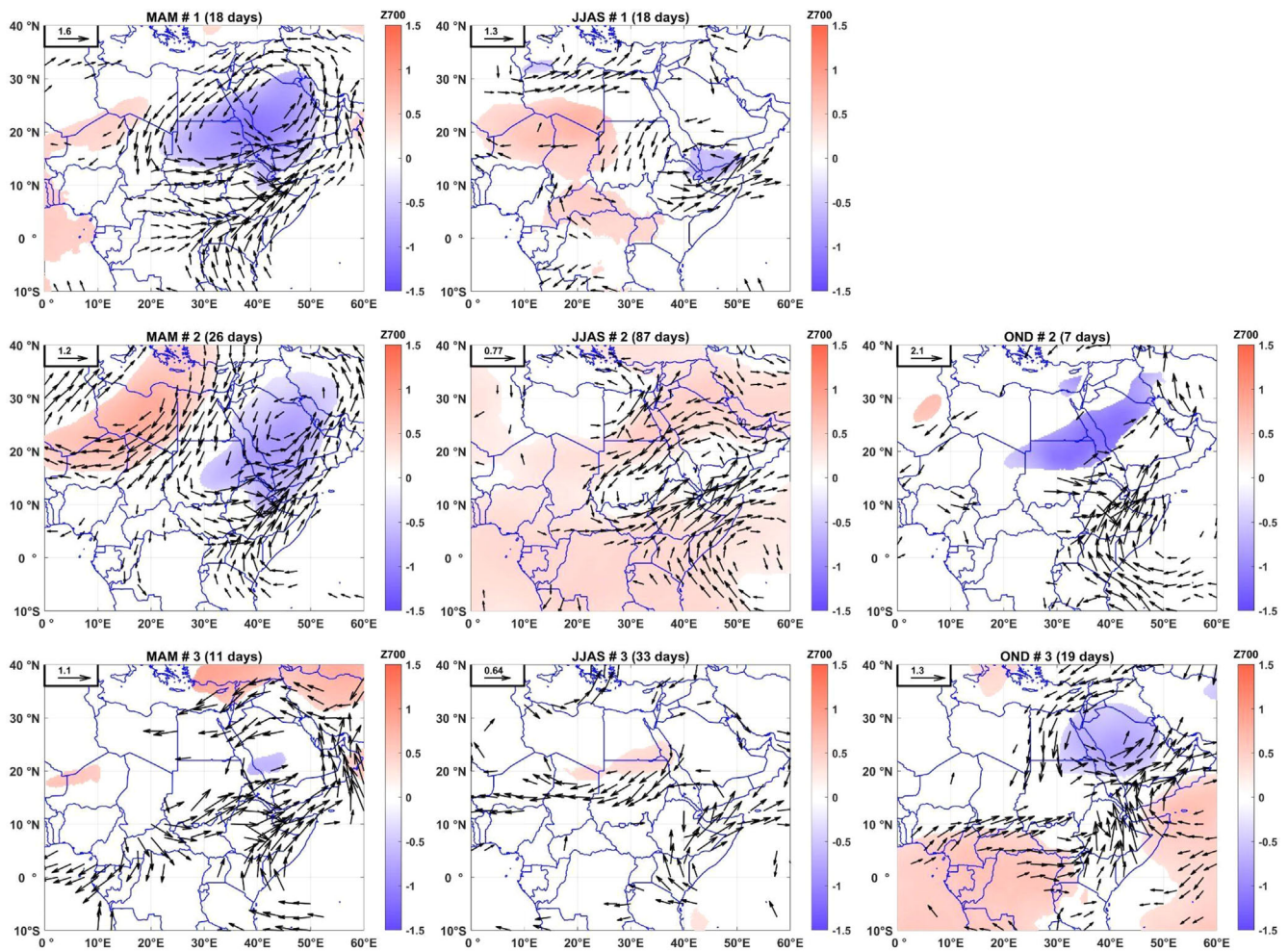


FIGURE 7 Composite analysis of geopotential height (shadings) and wind speed (arrows) at 700 hPa for the intense, southwestern and eastern clusters in the MAM, JJAS and OND seasons. Only the significant anomalies ($p < 0.05$, Student's t test) are displayed [Colour figure can be viewed at [wileyonlinelibrary.com](https://onlinelibrary.wiley.com/terms-and-conditions)]

margin of upper westerlies in JF and MAM (Figure 6). The wave pattern is quite similar for the three clusters (Figures 7 and 8), denoting that the dominant driver of most MAM rainfall events is associated with an activation of the Red Sea trough. However, the wave train has a more northerly direction for cluster #3 (“eastern”) than for clusters #1–2 (“intense” and “southwestern”), whose wave trains trace their origin over the Mediterranean and Europe (Figure 8).

The JJAS events, at 700 hPa, bear some similarities with MAM, showing a cyclonic anomaly associated with an anomalous low over the southern Red Sea, but contrary to MAM it is loosely related to the midlatitude circulation (Figure 7). This low drives an anomalous southwesterly flow over the Gulf of Aden, suggesting a thicker than normal and northward-shifted Indian monsoon flow at 700 hPa (especially for the southwestern cluster). In the upper troposphere (200 hPa; Figure 8), the circulation anomalies are very different from those of

the MAM season, with large similarities between the three clusters. Northerly anomalies prevail from the southern Red Sea to Kenya, veering to easterlies over Central Africa. Such an upper tropospheric outflow from summer hemisphere convection areas towards the winter hemisphere was found in many tropical regions with an upper easterly flow (Kiladis & Weickmann, 1997), which is the case of Djibouti in JJAS (Figure 6). It is a response to anomalous convection rather than its driver.

In OND, cluster #1 contains too few events for a composite to be computed. At 700 hPa, the “southwestern” and “eastern” clusters again show patterns reminiscent of those of the two previous seasons (Figure 7), with a trough over the northern Red Sea and an anomalous southerly flow over Djibouti. The connection with the extratropical circulation is not as clear as in MAM. The 200 hPa anomalies are weak for the “southwestern” cluster, but better defined for the “eastern” cluster, with uniformly positive anomalies in the Tropics, and an

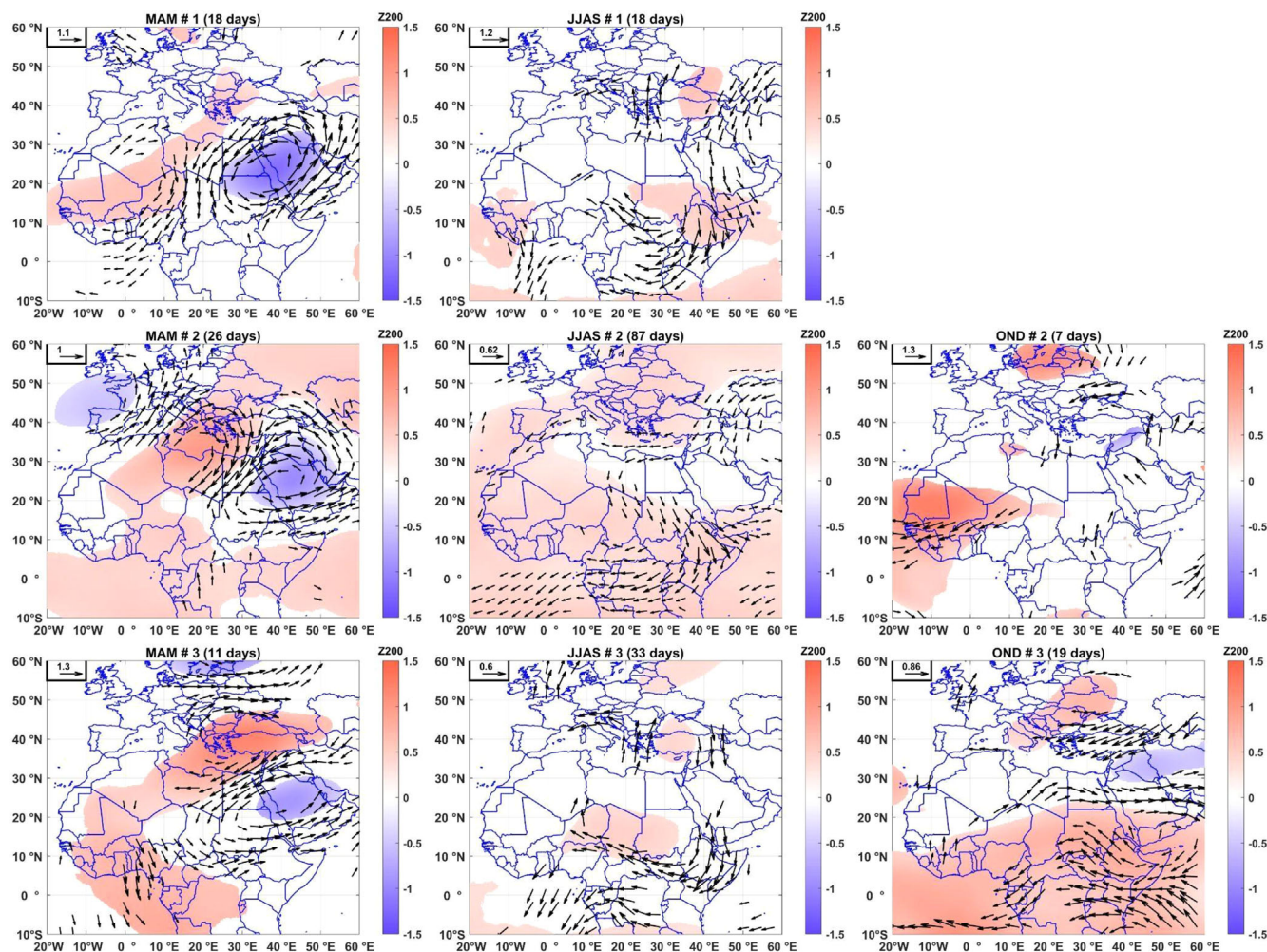


FIGURE 8 Composite analysis of geopotential height (shadings) and wind speeds (arrows) at 200 hPa for the intense, southwestern and eastern clusters in the MAM, JJAS and OND seasons. Only the significant anomalies ($p < 0.05$, Student's t test) are displayed [Colour figure can be viewed at wileyonlinelibrary.com]

anticyclonic anomaly over the Gulf of Aden, driving enhanced easterlies along the equator.

Figure 9 illustrates significant anomalies of precipitable water, vertically integrated moisture transport and outgoing longwave radiation flux for each cluster. Although the atmospheric circulation anomalies are again partly season- and cluster-dependent, there is a common pattern across all the composites of enhanced precipitable water and moisture convergence over the Republic of Djibouti, the latter mainly fed by a flow from the Indian Ocean.

In MAM, convergence between a southerly moisture flow from the Indian Ocean and a westerly flow from Ethiopia and Sudan is observed over the GHA. This drives a southwesterly moisture flow towards the Persian/Arabian Gulf, along the southeast margin of the RST shown in Figure 8. This convergence is associated with rising air in the mid troposphere (at 500 hPa; see Figure S4). A tilted band of positive precipitable

water and negative OLR anomalies is clearly shown between equatorial Africa and Iran while passing through Djibouti (Figure 9). This feature is characteristic of the tropical plumes (Knippertz & Martin, 2007), which are elongated high-level cloud bands, often associated with thunderstorms and atmospheric disturbances, which connect the Tropics and extratropics. This confirms that tropical–extratropical interactions are at the origin of most of the rainfall in Djibouti during this season.

In JJAS, the precipitable water and OLR anomalies do not show the tilted, elongated pattern of the MAM season anymore. Instead, Djibouti lies in a region of shear between the southwesterly moisture anomalies linked to the Indian monsoon (bringing moist air from the Indian Ocean), and the easterly anomalies found over the Red Sea and Sudan. Enhanced convection as suggested by the negative OLR anomalies is found over a region including Yemen and the northern Ethiopian Highlands, though they are more localized for the eastern

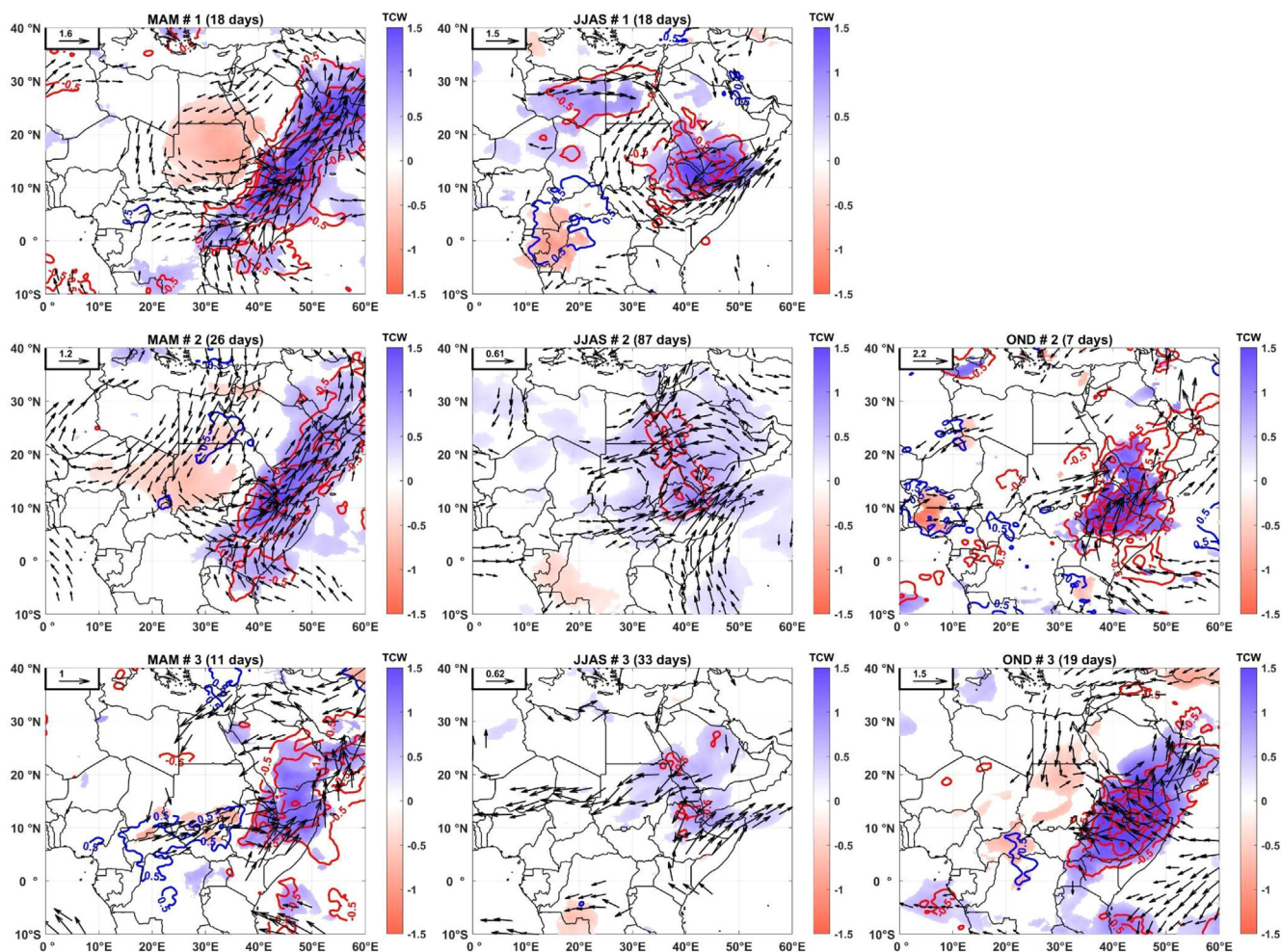


FIGURE 9 Composite analysis of precipitable water (shadings), outgoing longwave radiation flux (contours) and vertically integrated moisture transport (arrows) for the intense, southwestern and eastern clusters in the MAM, JJAS and OND seasons. Only the significant anomalies ($p < 0.05$, Student's t test) are displayed [Colour figure can be viewed at [wileyonlinelibrary.com](https://onlinelibrary.wiley.com/terms-and-conditions)]

cluster. Cluster #2 additionally shows distinct moisture convergence over Djibouti between the southerly flow from the Indian Ocean and the westerly flow from Central Africa.

In OND, most rainy events result from moisture advection (Figure 9) from the Western Indian Ocean favoured by positive phases of the Indian Ocean Dipole (Saji et al., 1999): 41% of the 29 rain events in the intense, southwestern and eastern clusters in OND, occurred in the positive phase of the IOD and only 17% in the negative phase. OLR and precipitable water show very strong anomalies over Djibouti and East Africa. The pattern is slightly reminiscent of that of MAM, with a tilt from southwest to northeast, but it is not as elongated as that of the tropical plumes found in MAM, as the spread does not extend beyond Arabia. Moisture convergence is also found over Djibouti between the flows from the Indian Ocean and those coming from the west via Sudan (cluster #2) and the north via the Red Sea (cluster #3).

3.3.3 | Case studies

The methodology used in the previous sections does not allow us to assess whether all days presenting similar rainfall conditions (and therefore regrouped into a single, coherent class) all result from similar rain-bearing mechanisms. In order to further stress that point, this subsection focuses on two selected case studies (12 April 2004 and 19 May 2018), both ascribed to the intense rainfall cluster for MAM. These days were chosen because they correspond to high-impact weather events (e.g., Marsigli et al., 2021), which were identified as primarily important by the World Meteorological Organization due to their increasing intensity and frequency under climate change. In order to quantify to which extent they differ from the average atmospheric circulation anomalies associated with intense rainfall days in MAM, Figure S5 shows the distance between the anomalous atmospheric pattern of each day and the MAM

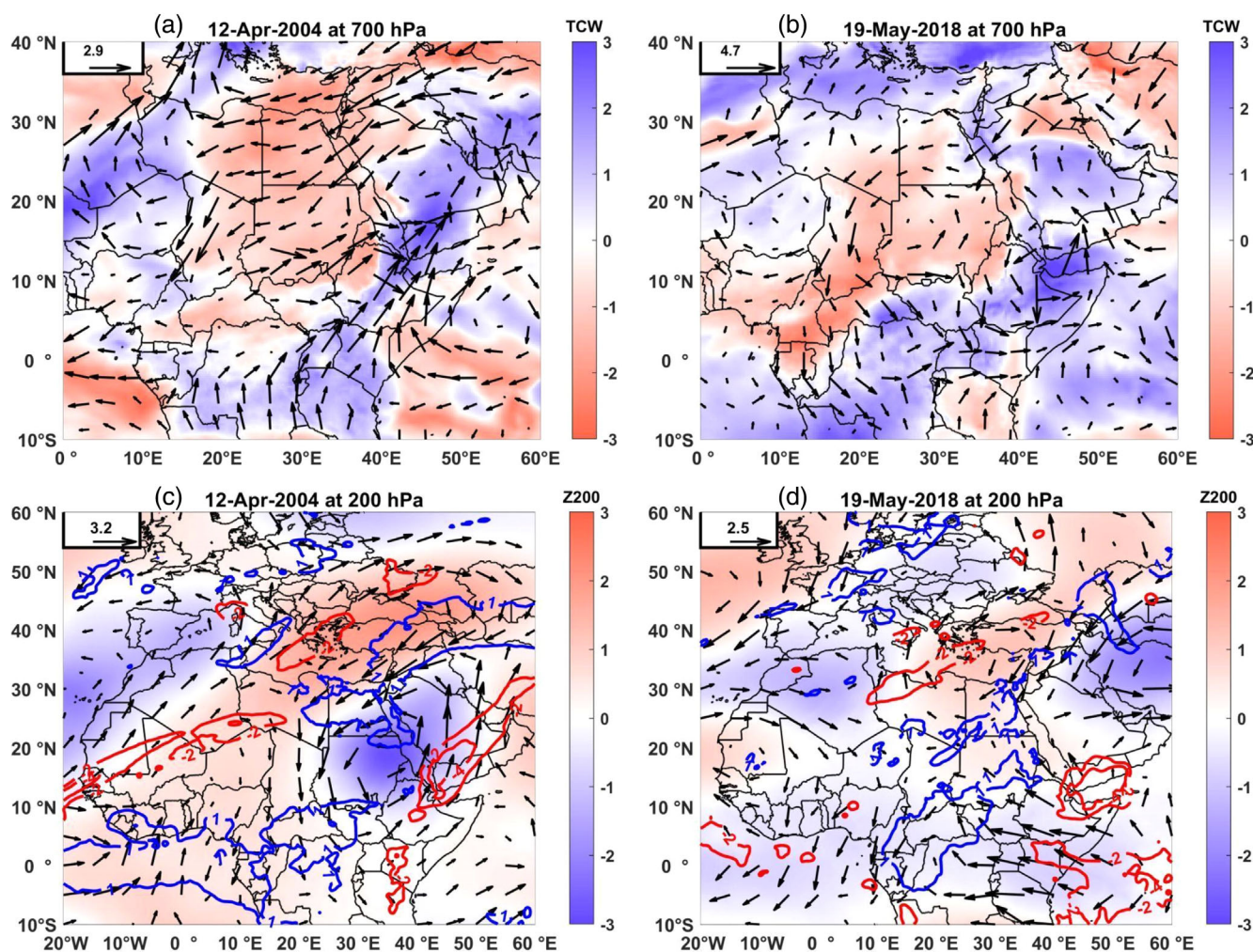


FIGURE 10 Composite analysis of precipitable water (shadings of (a) and (b)), geopotential height (shadings of (c) and (d)), outgoing longwave radiation flux (contour lines of (c) and (d)) and wind speed (arrows) corresponding to the 12 April 2004 and 19 May 2018 at 700 and 200 hPa pressure levels [Colour figure can be viewed at [wileyonlinelibrary.com](https://onlinelibrary.wiley.com/terms-and-conditions)]

cluster centroid for the 700 and 200 hPa fields, on the x-axis and y-axis, respectively.

The first case (12 April 2004) is among the closest days to the centroid of the intense rainfall cluster in MAM season. This day is part of a 4-day spell of torrential rains in Djibouti (11–14 April 2004 with 108 mm recorded at Djibouti Airport station) resulting in flash floods in many areas, predominantly affecting the Ambouli Wadi catchment (one of the country's largest), whose aquifer supplies Djibouti City's drinking water (Omar et al., 2023). It is estimated that approximately 300 people died; 600 houses were destroyed and another 100 inundated; 3000 persons were made homeless; and the lives of a total of 100,000 persons were affected (World Health Organization, 2004). Figure 10 shows that, on 12 April 2004, a trough was located over the Red Sea and Arabia at 200 and 700 hPa, a feature that more broadly characterizes the intense rainfall cluster

when it occurs in MAM (see Figures 8 and 9). The development of a tropical plume is also observed (see TCW and OLR anomalies), associated with rising motion and a strong moisture flow from East Africa to Arabia. This causes convergence of humidity and very high precipitable water anomalies over Djibouti which are the causes of the rains of that day. Therefore, these elements (Red Sea trough, tropical plume, humidity convergence over Djibouti, ...) indicate strong similarity between the synoptic atmospheric circulation of this day and that of the centroid of the intense cluster in the MAM season.

Another high-impact weather event is that of 19 May 2018. By contrast to the previous case study, this day is among the most dissimilar ones with respect to the centroid of the intense cluster in MAM. It coincides with the passage of the tropical cyclone Sagar which hit Djibouti on 19–20 May 2018 (with 110 mm recorded at Djibouti Airport station), causing severe flooding,

destruction of infrastructure (50% of Djibouti City was affected), houses (5–10,000 families or 25–50,000 people) and impoverishing the means of subsistence of the communities (Cherel et al., 2020; United Nations, 2018). For that day, Figure 10 shows a (clockwise) cyclonic rotation at 700 hPa over Djibouti, together with an anti-clockwise rotation at 200 hPa, which are characteristic features of tropical cyclones in the Northern Hemisphere. The presence of very high amounts of precipitable water, with moisture originating from the Indian Ocean, is also noted. Thus, the synoptic pattern responsible for the heavy rains in Djibouti is quite different from that of the centroid of the intense cluster for the MAM season. Although some similarities persist with the centroid (e.g., 700 hPa westerlies over equatorial Eastern Africa), this weather event does not seem to involve direct energy or mass transfers between the tropical and the extratropical circulations. Nonetheless, tropical–temperate interactions remain the main driver of most intense rains over Djibouti in MAM, since tropical disturbances such as that found on 19 May 2018 are very unusual features, to date, in the Gulf of Aden.

4 | CONCLUSION

This study provides for the first time a description of the atmospheric drivers of rainfall events at daily timescale in the Republic of Djibouti. For this purpose, we have exploited multiple data sources: 36 rain gauges, 4 gridded datasets of satellite rainfall estimates and ERA5 atmospheric reanalysis data.

A thorough evaluation was undertaken both in terms of occurrence and intensity of daily rainfall between the estimations of the satellite products and the rain gauges data over their common period (2013–2020). The analysis shows that the most robust way to detect observed rainfall events is to use all four satellite products in consensus. Despite the overall good performance of the consensus detection, it has some non-negligible limitations, especially during the rather dry JF season. This could be due to the nature of the rain-bearing systems in this season (cold fronts) which can be difficult to capture with the infrared imagery used by satellite products.

A multiproduct Agglomerative Hierarchical Clustering of the daily rain events detected in consensus by the four satellite products over their common period (2001–2020) shows the existence of four clusters of rain events in Djibouti (intense, southwestern, eastern and moderate). These clusters are distinguished, among other things, by the intensity, spatial pattern and extension of their rainfall event. The composite analysis of the days

ascribed to each cluster shows that the atmospheric circulation anomalies are more season dependent than cluster dependent, but there are nonetheless significant differences between clusters.

Our analyses identify a diversity of atmospheric rain-bearing mechanisms in Djibouti. The rains in the MAM season are mainly forced by upper-tropospheric wave trains which activate the Red Sea trough and favours tropical–extratropical interactions illustrated by the tropical plumes. Finally, in the OND season, most rainy events result from moisture advection from the Western Indian Ocean favoured by positive phases of the Indian Ocean Dipole. Relationships between the frequency of events in each cluster and both ENSO and the North Atlantic Oscillation have also been examined, but did not show consistently significant results. This is partly due to the JJAS season, the rains are associated with anomalies in the monsoon flow (enhanced southerlies, converging with enhanced westerlies across Ethiopia) resulting in stronger convection around the southern Red Sea. Upper-tropospheric anomalies are merely a response to the anomalous convection, to the short period of time under investigation (20 years), which does not enable to document interannual variations with sufficient statistical robustness.

The differences between the clusters consist of second-order variations around these general patterns, which involve for instance in MAM different pathways for the upper-tropospheric wave trains. Nevertheless, the importance of these quite subtle variations is such that they can directly influence the geography, intensity and frequency of the seasonal rainfall events. For example, a meridional (tilted) orientation of the wave trains results in the MAM rainfall events being located in the eastern (southwestern) part of the country. A strong implication is that, besides the identification of the broad-scale atmospheric patterns favourable to rainfall occurrence over the country, a skilful prediction of the location of the most intense rains requires a close understanding, monitoring and eventually forecasting, of such second-order circulation anomalies. Finally, some heavy rainfall events demarcate markedly from the canonical atmospheric patterns described above. This includes the rare occurrence of tropical cyclones reaching the Gulf of Aden.

The above description of the atmospheric mechanisms at the origin of the rains in Djibouti can be useful for meteorological applications such as an improved prediction of the rainy events of the country. Given the vulnerability of Djibouti and the East African region to climate change, it is crucial to consider future changes in the regional climate, in order to improve resilience and define robust adaptation strategies. In order to obtain realistic rainfall projections, it is nonetheless essential to

understand their physical causes and verify their correct representation by climate models.

AUTHOR CONTRIBUTIONS

Moussa Mohamed Waberi: Conceptualization; investigation; software; writing – review and editing; writing – original draft. **Pierre Camberlin:** Conceptualization; methodology; supervision; project administration; writing – original draft. **Benjamin Pohl:** Validation; investigation; supervision; writing – original draft. **Omar Assowe Dabar:** Formal analysis; funding acquisition; resources; conceptualization.

ACKNOWLEDGEMENTS

The authors would like the National Meteorological Agency (ANM) of the Republic of Djibouti for providing the observed data. The authors would like to thank the Centre d'Etudes et de Recherches de Djibouti (CERD) and Campus France (French government doctoral scholarship) for their financial support. Calculations were performed using HPC resources from DNUM CCUB (Centre de Calcul de l'Université de Bourgogne).

ORCID

Moussa Mohamed Waberi  <https://orcid.org/0000-0003-2183-4808>

Pierre Camberlin  <https://orcid.org/0000-0003-4896-2332>

Benjamin Pohl  <https://orcid.org/0000-0002-9339-797X>

Omar Assowe Dabar  <https://orcid.org/0000-0002-4095-3194>

REFERENCES

- Abdou, F.S. (1990) El-NINO et la variabilité des précipitations dans la République de Djibouti. *Sciences & Techniques (Djibouti)*, 4, 19–30.
- Almazroui, M., Alobaidi, M., Saeed, S., Mashat, A. & Assiri, M. (2018) The possible impact of the circumglobal wave train on the wet season dust storm activity over the northern Arabian Peninsula. *Climate Dynamics*, 50(5), 2257–2268. Available from: <https://doi.org/10.1007/s00382-017-3747-1>
- Assowe Dabar, O., Adan, A.-B., Mahdi Ahmed, M., Awaleh, M., Waberi, M., Camberlin, P. et al. (2022) Evolution and trends of meteorological drought and wet events over the Republic of Djibouti from 1961 to 2021. *Climate*, 10, 1–27. Available from: <https://doi.org/10.3390/cli10100148>
- Assowe Dabar, O., Camberlin, P., Pohl, B., Mohamed Waberi, M., Osman Awaleh, M. & Silah-Eddine, S. (2021) Spatial and temporal variability of rainfall over the Republic of Djibouti from 1946 to 2017. *International Journal of Climatology*, 41(4), 2729–2748. Available from: <https://doi.org/10.1002/joc.6986>
- Atif, R.M., Almazroui, M., Saeed, S., Abid, M.A., Islam, M.N. & Ismail, M. (2020) Extreme precipitation events over Saudi Arabia during the wet season and their associated teleconnections. *Atmospheric Research*, 231, 104655. Available from: <https://doi.org/10.1016/j.atmosres.2019.104655>
- Beau, A., Bouhris, E. & Bergès, R. (1976) Aperçu de climatologie dynamique du territoire français des Afars et des Issas. *Météo*, 6, 63–68.
- Beck, H.E., Vergopolan, N., Pan, M., Levizzani, V., van Dijk, A.I.J.M., Weedon, G.P. et al. (2017) Global-scale evaluation of 22 precipitation datasets using gauge observations and hydrological modeling. *Hydrology and Earth System Sciences*, 21(12), 6201–6217. Available from: <https://doi.org/10.5194/hess-21-6201-2017>
- Beck, H.E., Wood, E.F., Pan, M., Fisher, C.K., Miralles, D.G., van Dijk, A.I.J.M. et al. (2019) MSWEP V2 global 3-hourly 0.1° precipitation: methodology and quantitative assessment. *Bulletin of the American Meteorological Society*, 100(3), 473–500. Available from: <https://doi.org/10.1175/BAMS-D-17-0138.1>
- Bekele-Biratu, E., Thiaw, W.M. & Korecha, D. (2018) Sub-seasonal variability of the Belg rains in Ethiopia. *International Journal of Climatology*, 38(7), 2940–2953. Available from: <https://doi.org/10.1002/joc.5474>
- Branstator, G. (2002) Circumglobal teleconnections, the jet stream waveguide, and the North Atlantic oscillation. *Journal of Climate*, 15(14), 1893–1910. Available from: [https://doi.org/10.1175/1520-0442\(2002\)015<1893:CTTJSW>2.0.CO;2](https://doi.org/10.1175/1520-0442(2002)015<1893:CTTJSW>2.0.CO;2)
- Camberlin, P. (2018) Climate of eastern Africa. In: *Oxford research encyclopedia of climate science*. Oxford: Oxford University Press.
- Camberlin, P., Barraud, G., Bigot, S., Dewitte, O., Makanzu Imwangana, F., Maki Mateso, J.C. et al. (2019) Evaluation of remotely sensed rainfall products over Central Africa. *Quarterly Journal of the Royal Meteorological Society*, 145(722), 2115–2138. Available from: <https://doi.org/10.1002/qj.3547>
- Cattani, E., Merino, A. & Levizzani, V. (2020) Rainfall trends in East Africa from an ensemble of IR-based satellite products. In: Levizzani, V., Kidd, C., Kirschaum, D.B., Kummerow, C.D., Nakamura, K. & Turk, F.J. (Eds.) *Satellite precipitation measurement*, Vol. 2. Cham: Springer, pp. 791–817.
- Cherel, J.-P., Omar Ali, B., Nour Ayeih, M. & Vinet, F. (2020) Activités cycloniques et nouveaux risques dans le golfe d'Aden. *EchoGéo*, 2020, 51. Available from: <https://doi.org/10.4000/echogeo.18859>
- Copernicus Climate Change Service. (2017) *ERA5: fifth generation of ECMWF atmospheric reanalyses of the global climate*. London: Copernicus Climate Change Service Climate Data Store (CDS). Available from: <https://cds.climate.copernicus.eu/cdsapp#!/home> [Accessed 26th January 2023]
- de Vries, A.J., Feldstein, S.B., Riemer, M., Tyrlis, E., Sprenger, M., Baumgart, M. et al. (2016) Dynamics of tropical–extratropical interactions and extreme precipitation events in Saudi Arabia in autumn, winter and spring. *Quarterly Journal of the Royal Meteorological Society*, 142(697), 1862–1880. Available from: <https://doi.org/10.1002/qj.2781>
- Ding, Q. & Wang, B. (2005) Circumglobal teleconnection in the Northern Hemisphere summer. *Journal of Climate*, 18(17), 3483–3505. Available from: <https://doi.org/10.1175/JCLI3473.1>
- Dinku, T., Funk, C., Peterson, P., Maidment, R., Tadesse, T., Gadain, H. et al. (2018) Validation of the CHIRPS satellite rainfall estimates over eastern Africa. *Quarterly Journal of the Royal Meteorological Society*, 144, 292–312. Available from: <https://doi.org/10.1002/qj.3244>
- Evan, A.T. & Camargo, S.J. (2011) A climatology of Arabian Sea cyclonic storms. *Journal of Climate*, 24(1), 140–158. Available from: <https://doi.org/10.1175/2010JCLI3611.1>

- Flohn, H. (1965) Klimaprobleme am Roten Meer. *Erdkunde*, 19(3), 179–191.
- Funk, C., Peterson, P., Landsfeld, M., Pedreros, D., Verdin, J., Shukla, S. et al. (2015) The climate hazards infrared precipitation with stations—a new environmental record for monitoring extremes. *Scientific Data*, 2(1), 150066. Available from: <https://doi.org/10.1038/sdata.2015.66>
- Gebrechorkos, S.H., Hülsmann, S. & Bernhofer, C. (2018) Evaluation of multiple climate data sources for managing environmental resources in East Africa. *Hydrology and Earth System Sciences*, 22(8), 4547–4564. Available from: <https://doi.org/10.5194/hess-22-4547-2018>
- Habtemichael, A. & Pedgley, D.E. (1974) Synoptic case-study of spring rains in Eritrea. *Archiv für Meteorologie, Geophysik und Bioklimatologie, Serie A*, 23(3), 285–296. Available from: <https://doi.org/10.1007/BF02247268>
- Hersbach, H., Bell, B., Berrisford, P., Hirahara, S., Horányi, A., Muñoz-Sabater, J. et al. (2020) The ERA5 global reanalysis. *Quarterly Journal of the Royal Meteorological Society*, 146(730), 1999–2049. Available from: <https://doi.org/10.1002/qj.3803>
- Houmed-Gaba, A. (2009) *Hydrogéologie des milieux volcaniques sous climat aride: caractérisation sur site expérimental et modélisation numérique de l'aquifère basaltique de Djibouti (Corne de l'Afrique)*. PhD thesis, Université de Poitiers. Available from <https://www.theses.fr/2009POIT2266>
- Jury, M.R. (2011) Meteorological scenario of Ethiopian floods in 2006–2007. *Theoretical and Applied Climatology*, 104(1), 209–219. Available from: <https://doi.org/10.1007/s00704-010-0337-0>
- Jury, M.R. (2016) Convective outbreak over the Red Sea and downstream easterly waves. *Earth Interactions*, 20(21), 1–17. Available from: <https://doi.org/10.1175/EI-D-16-0009.1>
- Kiladis, G.N. & Weickmann, K.M. (1997) Horizontal structure and seasonality of large-scale circulations associated with sub-monthly tropical convection. *Monthly Weather Review*, 125(9), 1997–2013. Available from: [https://doi.org/10.1175/1520-0493\(1997\)125<1997:HSASOL>2.0.CO;2](https://doi.org/10.1175/1520-0493(1997)125<1997:HSASOL>2.0.CO;2)
- Kimani, M.W., Hoedjes, J.C.B. & Su, Z. (2017) An assessment of satellite-derived rainfall products relative to ground observations over East Africa. *Remote Sensing*, 9(5), 430. Available from: <https://doi.org/10.3390/rs9050430>
- Knippertz, P. & Martin, J.E. (2007) A Pacific moisture conveyor belt and its relationship to a significant precipitation event in the semi-arid southwestern United States. *Weather and Forecasting*, 22(1), 125–144. Available from: <https://doi.org/10.1175/WAF963.1>
- Marsigli, C., Ebert, E., Ashrit, R., Casati, B., Chen, J., Coelho, C.A.S. et al. (2021) Review article: observations for high-impact weather and their use in verification. *Natural Hazards and Earth System Sciences*, 21(4), 1297–1312. Available from: <https://doi.org/10.5194/nhess-21-1297-2021>
- Mekonnen, A. & Rossow, W.B. (2018) The interaction between deep convection and easterly wave activity over Africa: convective transitions and mechanisms. *Monthly Weather Review*, 146(6), 1945–1961. Available from: <https://doi.org/10.1175/MWR-D-17-0217.1>
- Nicholson, S.E. (1996) A review of climate dynamics and climate variability in Eastern Africa. In: *The limnology, climatology and paleoclimatology of the East African lakes*. Boca Raton: CRC Press. 25–56. Available from: <https://doi.org/10.1201/9780203748978-2>
- Nicholson, S.E. (2014) A detailed look at the recent drought situation in the Greater Horn of Africa. *Journal of Arid Environments*, 103, 71–79. Available from: <https://doi.org/10.1016/j.jaridenv.2013.12.003>
- Nicholson, S.E. (2017) Climate and climatic variability of rainfall over eastern Africa. *Reviews of Geophysics*, 55(3), 590–635. Available from: <https://doi.org/10.1002/2016RG000544>
- Omar, G.M., Paturel, J.E., Salles, C., Mahé, G., Jalludin, M., Satgé, F. et al. (2023) Evaluation of rainfall products in semi-arid areas: application to the southeast of the Republic of Djibouti and a focus on the Ambouli catchment. *Water*, 15(12), 2168. Available from: <https://doi.org/10.3390/w15122168>
- Ozer, P. & Mahamoud, A. (2013) Recent extreme precipitation and temperature changes in Djibouti City (1966–2011). *Journal of Climatology*, 2013, 1–8. Available from: <https://doi.org/10.1155/2013/928501>
- Palmer, P.I., Wainwright, C.M., Dong, B., Maidment, R.I., Wheeler, K.G., Gedney, N. et al. (2023) Drivers and impacts of eastern African rainfall variability. *Nature Reviews Earth & Environment*, 4(4), 254–270. Available from: <https://doi.org/10.1038/s43017-023-00397-x>
- Pedgley, D.E. (1966) The Red Sea convergence zone. *Weather*, 21(10), 350–358. Available from: <https://doi.org/10.1002/j.1477-8696.1966.tb02776.x>
- République de Djibouti. (2011) Evaluation des Dommages, Pertes et Besoins suite à la Sécheresse. *Gouvernement de la République de Djibouti/Global Forum for Disaster Risk Reduction (GFDRR)*. https://www.gfdr.org/sites/default/files/publication/Djibouti_PDNA.pdf
- Saeed, S., Müller, W.A., Hagemann, S. & Jacob, D. (2011) Circum-global wave train and the summer monsoon over northwestern India and Pakistan: the explicit role of the surface heat low. *Climate Dynamics*, 37(5), 1045–1060. Available from: <https://doi.org/10.1007/s00382-010-0888-x>
- Saeed, S., Van Lipzig, N., Müller, W.A., Saeed, F. & Zanchettin, D. (2014) Influence of the circumglobal wave-train on European summer precipitation. *Climate Dynamics*, 43(1), 503–515. Available from: <https://doi.org/10.1007/s00382-013-1871-0>
- Said Chiré, A. (2015) De la production sociale de la ville à la production de vulnérabilités, l'exemple de la ville de Djibouti. *Territory in Movement Journal of Geography and Planning*, 2015, 27–28. Available from: <https://doi.org/10.4000/tem.3157>
- Saji, N.H., Goswami, B.N., Vinayachandran, P.N. & Yamagata, T. (1999) A dipole mode in the tropical Indian Ocean. *Nature*, 401(6751), 360–363. Available from: <https://doi.org/10.1038/43854>
- Samman, A.E. & Gallus, W.A., Jr. (2018) A climatology of the winter low-level jet over the Red Sea. *International Journal of Climatology*, 38(15), 5505–5521. Available from: <https://doi.org/10.1002/joc.5742>
- Satgé, F., Defrance, D., Sultan, B., Bonnet, M.-P., Seyler, F., Rouché, N. et al. (2020) Evaluation of 23 gridded precipitation datasets across West Africa. *Journal of Hydrology*, 581, 124412. Available from: <https://doi.org/10.1016/j.jhydrol.2019.124412>
- Tan, J., Huffman, G.J., Bolvin, D.T. & Nelkin, E.J. (2019) IMERG V06: changes to the morphing algorithm. *Journal of Atmospheric and Oceanic Technology*, 36(12), 2471–2482. Available from: <https://doi.org/10.1175/JTECH-D-19-0114.1>
- Terry, J.P. & Gienko, G. (2019) Quantitative observations on tropical cyclone tracks in the Arabian Sea. *Theoretical and Applied*

- Climatology*, 135(3), 1413–1421. Available from: <https://doi.org/10.1007/s00704-018-2445-1>
- Tiwari, G., Kumar, P., Javed, A., Mishra, A.K. & Routray, A. (2022) Assessing tropical cyclones characteristics over the Arabian Sea and Bay of Bengal in the recent decades. *Meteorology and Atmospheric Physics*, 134(3), 44. Available from: <https://doi.org/10.1007/s00703-022-00883-9>
- UNDP/UNSO. (1997) *Aridity zones and dryland populations: an assessment of population levels in the world's drylands with particular reference to Africa*. New York, NY: UNDP Office to Combat Desertification and Drought (UNSO).
- United Nations. (2018) *Djibouti Cyclone Sagar et inondations: Evaluation rapide des besoins humanitaires*. Available from: <https://djibouti.un.org/sites/default/files/2020-11/Djibouti%20Evaluation%20Besoins%20Humanitaires%20Cyclone%20Sagar%20-%20Mai%202018.pdf>
- Wheeler, M.C. & Hendon, H.H. (2004) An all-season real-time multivariate MJO index: development of an index for monitoring and prediction. *Monthly Weather Review*, 132(8), 1917–1932. Available from: [https://doi.org/10.1175/1520-0493\(2004\)132<1917:aarmmi>2.0.co;2](https://doi.org/10.1175/1520-0493(2004)132<1917:aarmmi>2.0.co;2)
- Williams, A.P., Funk, C., Michaelsen, J., Rauscher, S.A., Robertson, I., Wils, T.H.G. et al. (2012) Recent summer precipitation trends in the Greater Horn of Africa and the emerging role of Indian Ocean sea surface temperature. *Climate Dynamics*, 39(9), 2307–2328. Available from: <https://doi.org/10.1007/s00382-011-1222-y>
- World Health Organization. (2004) *Assessment report on the April 2004 floods: Republic of Djibouti*. Available from: https://www.preventionweb.net/files/559_7958.pdf
- Xie, P. & Arkin, P.A. (1996) Analyses of global monthly precipitation using gauge observations, satellite estimates, and numerical model predictions. *Journal of Climate*, 9(4), 840–858. Available from: [https://doi.org/10.1175/1520-0442\(1996\)009%3C0840:AOGMPU%3E2.0.CO;2](https://doi.org/10.1175/1520-0442(1996)009%3C0840:AOGMPU%3E2.0.CO;2)
- Yang, W., Seager, R., Cane, M.A. & Lyon, B. (2015) The annual cycle of East African precipitation. *Journal of Climate*, 28(6), 2385–2404. Available from: <https://doi.org/10.1175/JCLI-D-14-00484.1>

SUPPORTING INFORMATION

Additional supporting information can be found online in the Supporting Information section at the end of this article.

How to cite this article: Waberi, M. M., Camberlin, P., Pohl, B., & Dabar, O. A. (2023). Atmospheric drivers of rainfall events in the Republic of Djibouti. *International Journal of Climatology*, 1–20. <https://doi.org/10.1002/joc.8299>